Sub Topic: Reaction kinetics

2022 Spring Technical Meeting
Central States Section of The Combustion Institute
May 15–17, 2022
Detroit, Michigan

A Study of the Effects of Steam Addition on Ammonia Hydrogen Air Combustion

Sreetam Bhaduri and Jay P. Gore*

School of Mechanical Engineering, Purdue University, West Lafayette, 47907, USA
**Corresponding Author Email: bhaduri@purdue.edu*

ABSTRACT: Ammonia and hydrogen are potential fuels for eliminating direct CO_2 emissions considering climate change. The volumetric energy density of ammonia is 11,333 kJ/m^3, and the volumetric energy density of hydrogen is 2,101 kJ/m^3. The ignition energy of ammonia is 8 MJ, and the ignition energy of hydrogen is 0.08 MJ. Ammonia hydrogen mixtures in the right proportions may serve as a practical fuel if the additional challenge related to NO_x emissions is addressed. Steam addition is an effective means of controlling the increases in NO_x emissions resulting from either the fuel nitrogen and or the high temperatures resulting from the energy density. A computational study of turbulent ammonia + hydrogen burning with air + steam in axisymmetric opposed flow flame configurations is reported. The ANSYS Chemkin-Pro, a commercially available chemical kinetics code with the Konnov ammonia hydrogen-air reaction mechanism, is utilized. In this article, results are reported of combustion of ammonia and hydrogen with air and steam. Two mole fractions of ammonia in the fuel flow (0.9 and 1.0) and multiple mole fractions of steam (in the range 0.0 to 0.20) in the oxidizer flow in an opposed flow flame configuration at a constant mean pressure of 101 kPa and an initial fuel temperature of 298 K are considered. Six steam-air mixture temperatures in the range 473 K to 973 K for the multiple steam mole fractions are considered. The NO mass fractions decreased with the mole fraction of steam in the incoming oxidizer. Stable combustion is observed when a small amount of hydrogen is added.

Keywords: Ammonia, Hydrogen, Chemical Kinetics, NO_x Control.

INTRODUCTION: Carbon emissions is a burning issue that must be addressed. Combustion of fossil fuels contributes to significant greenhouse gas emissions [1]. The hydrocarbon fuels used for combustion can potentially be replaced with zero-carbon fuels such as ammonia (NH_3) and hydrogen (H_2). The nitrogen atom in the ammonia molecule is a potential contributor to NO_x emissions [2]. Additional challenges include the higher flashpoint and autoignition temperatures of ammonia (-33.4^o C and 651^o C compared to -42.7^o C and 280^o C of gasoline) [2]. The minimum ignition energies of hydrogen (0.018 MJ), gasoline (0.14 MJ), and ammonia (8 MJ) are between ~1 to 1.6 orders of magnitude different [2]. This makes hydrogen extremely easy to ignite and quite dangerous to store as fuel. An appropriate blend of hydrogen and ammonia could potentially be prepared for utilization in a gasoline engine to provide an acceptable combination of flashpoint, autoignition temperature, and autoignition energy while avoiding the CO_2 emissions and controlling the NO_x emissions to acceptable levels.

Yang et al. [3] conducted direct numerical simulations of combustion of ammonia and blended ammonia-hydrogen combustion in a constant volume chamber with a range of equivalence ratios at an initial temperature of 445 K and an initial pressure of 5.4 bar. For a 15% by volume blend of ammonia-hydrogen in comparison with unblended ammonia, the laminar flame speed

increased by almost 55% but the net production rate of NO increased by almost 96%. Goldmann et al. [4] studied flame flashback for an axisymmetric non-swirling jet flame burning H_2, NH_3, N_2, and O_2 mixtures at atmospheric pressure. A comparison of interest is between a flame that burns NH_3 with a flame that burns a 3:1 molecular mixture of H_2 and N_2. The addition of nitrogen increased the flashback propensity of all ammonia-hydrogen-air flames because of the reduction in the flame speed leading to flame stabilization near the burner rim and the associated heat transfer. Cellek [5] computed that ammonia addition shortened the flame length and lowered the flame temperature leading to a significant reduction in the NOx emissions from hydrogen-air flames.

Yu et al. [6] numerically studied the chemistry of ammonia-air combustion with a relatively low mole fraction of hydrogen in the fuel stream. As expected their results show that the overall flame temperature increased slightly with the increase in the heating value. The increases in the local temperatures led to corresponding increases in NH_2 and H_2NO radicals leading to corresponding increases in NO concentrations. Kanoshima et al. [7] numerically studied the effect of the initial pressure and temperature on ammonia-air combustion with boundary conditions stipulated to yield results that are relevant to internal combustion engines. The authors showed that the initial temperature of the reactants increased the rate of the chain branching reaction $H + O_2 = O + OH$ more significantly than the initial pressure.

Shen et al. [8] numerically investigated the effects of steam addition in hydrogen-ammonia-air combustion in a gas turbine combustor. The authors found that for mixtures containing less than 30% hydrogen, the flame thickness increased because of the decreases in the local fuel concentrations, however, the laminar flame speed did not increase. The NO emissions decreased with the decreases in the local equivalence ratio for a fixed hydrogen mole fraction but increased with increases in the hydrogen mole fraction leading to an overall non-monotonic behavior. Mashruk et al. [9] also reported that humidified hydrogen-ammonia-air combustion lowered the computational estimates of NO emissions. The concentrations of HONO and HNO radicals and NO_2 molecules affected the NO production rates. He et al. [10] found that under stoichiometric conditions, water significantly suppressed NO production by reducing the concentration of O radical in their numerical investigation of the effects of water addition in a stoichiometric flow reactor burning ammonia with air. For rich mixtures, the NO emissions production rate increased under rich mixture conditions due to increased OH radical concentrations.

The present study involves computations of non-premixed stagnation flames burning ammonia and a 90% ammonia 10% hydrogen mixture with air and air and 5%, 10%, 15%, 20% steam mixtures stabilized in a counterflow burner. The ANSYS Chemkin – Pro commercial software package is utilized. The bulk velocity and inlet temperature of the fuel flow are maintained constant at 0.5 m/s and 298 K. The bulk temperature of the oxidizer flow is varied between 473 K and 973 K with an interval of 100 K. A total of 60 operating conditions are studied with 40 conditions leading to stable flames with various temperatures and species concentrations and 20 conditions leading to extinction. The variations in axial velocities, flame temperatures, and the axial locations of the stagnation planes and the peak mole fractions of NO are studied to gain an understanding of the combustion process and to delineate the operating conditions of interest for deeper studies.

COUNTERFLOW BURNER: A schematic diagram of an opposed flow flame burner built for measuring flame temperatures with optical diagnostics with a precision of 1 K at 1000 K is

depicted in Fig. 1. The present simulations utilize the detailed geometry of this burner as a step towards utilizing the detailed measurements for validation of computational methods. The NH_3+H_2 mixture is upwards from the bottom and the H_2O+O_2+N_2 mixture flows downwards from the top. The distance between the top and the bottom inlets is 10 mm and the diameters of the two inlets are equal to 20 mm (Fig.1(a)). Both the NH_3+H_2 and the H_2O+O_2+N_2 inlets are shielded by an annular flow of N_2 to avoid room air entrainment as shown in Fig.1(b). The temperature, 298 K, and the bulk velocity, 0.5 m/s, of the NH_3+H_2 flow are maintained constant. Two fuel compositions $0.9NH_3$+$0.1H_2$ and $1.0NH_3$ +$0.0H_2$ are considered with the oxidizer temperatures varying between 473 K and 973 K. The 60 operating conditions resulting from these combinations are summarized in Table 1. The Konnov [11] reaction mechanism adopted by Xiao et al. [12] and Meyer and coworkers [13] is considered. Transient conservation equations consisting of mass, momentum, species, and energy are considered. The Konnov mechanism is more suitable for ammonia combustion under lean conditions [13].

Table 1 depicts the operating conditions for the flames considered in the present computations. Two inlet compositions of the fuel flow ($1.0NH_3$+$0.0H_2$, and $0.9NH_3$+$0.1H_2$) are shown in the first column. The inlet oxidizer flow compositions at each of the six inlet temperatures are depicted in the next three columns.

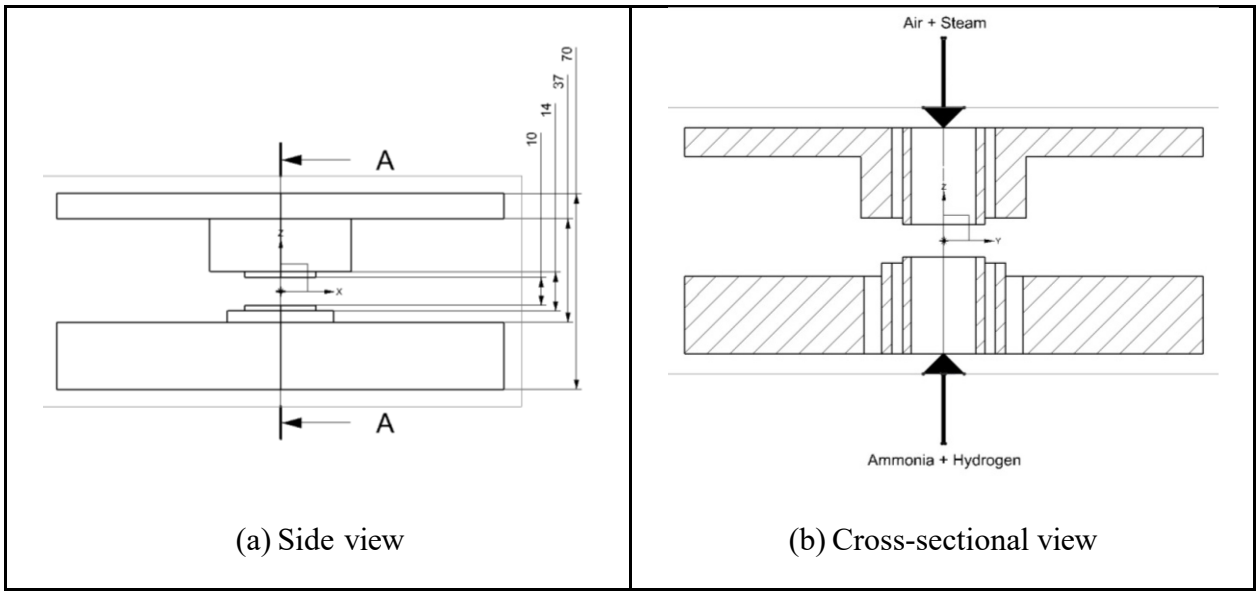

(a) Side view (b) Cross-sectional view

Fig.1. Schematic diagram of the counterflow burner

Sixty different sets of boundary conditions result from these combinations allowing a study of the effects of hydrogen addition to the fuel flow and of steam addition to the airflow of the structure and NO formation properties of the opposed flame flames. The oxidizer mixture velocities are calculated to result in a stoichiometric mixture upon complete mixing of the reactants and the products. This results in a value of the coefficient in the algebraic expression for the oxidizer velocity in the last column of Table 1 to be $n = \frac{T_{ox}-473}{100}$. The location of the stagnation surface and the scalar dissipation rate at the flame location is determined by the velocities of the two flows. However, the present results are representative of conditions of practical interest.

The species and energy conservation equations are solved with a multicomponent diffusion model using Chemkin-Pro and the boundary conditions prescribed from the inlet operating conditions summarized in Table 1. The diffusion flame introduces strong temperature gradients on both the fuel and the oxidizer side leading to increases in the species and thermal diffusivities. The Soret effect is considered in the thermal diffusivity model [14].

Table.1. Operating Conditions for the 60 flames with two ammonia-hydrogen fuel mixtures, five oxidizer-steam mixtures at oxidizer-steam inlet temperatures 473K, 573K, 673K, 773K, 873K, 973K

X_{H2}	X_{NH3}	X_{Steam}	X_{O2}	X_{N2}	v_{ox} (m/s)
0.1	0.9	0.00	0.21	0.79	$0.5825 + 0.1232n = 0.5825$
		0.05	0.20	0.75	$0.5930 + 0.1255n = 0.708$
		0.10	0.19	0.71	$0.6029 + 0.1276n = 0.8581$
		0.15	0.18	0.67	$0.6122 + 0.1297n = 1.0013$
		0.20	0.17	0.63	$0.6210 + 0.1316n$=1.1474
0.0	1.0	0.00	0.21	0.79	$0.6096 + 0.1205n = 0.6096$
		0.05	0.20	0.75	$0.6136 + 0.1297n = 0.7433$
		0.10	0.19	0.71	$0.6237 + 0.1321n = 0.8879$
		0.15	0.18	0.67	$0.6334 + 0.1341n = 1.0357$
		0.20	0.17	0.63	$0.6425 + 0.1361n = 1.1869$

RESULTS AND DISCUSSIONS: The effects of hydrogen addition to the ammonia and of steam addition to the preheated air on the peak temperatures, the locations of the stagnation plane, and the peak mass fractions of NO are considered.

Variation of peak temperature:

Figure 2(a) shows the peak flame temperatures for 10%H_2+ 90%NH_3 flames plotted as a function of the mole fraction of steam for the six different oxidizer flow temperatures. The peak temperatures for a total of 30 flames are depicted showing that the peak temperature increases from 2000 K to 2300 K when the air temperature is increased from 473K to 973 K. The peak temperature of the ammonia air flame is consistent with the results reported in Ref. [15]. The lower increase in the flame temperatures results from the higher specific heats of the products at their temperatures compared to those of the reactants at their temperature. Twenty nine of the thirty flames shown in Figure 2(a) do not show any evidence of extinction while one the thirty flames corresponding to 20% steam addition to the air shows extinction depicted by the peak temperature being equal to the inlet oxidizer temperature. The percentage of steam addition leading to extinction is of interest in practical applications and future experimental studies will assess the validity of this computed result.

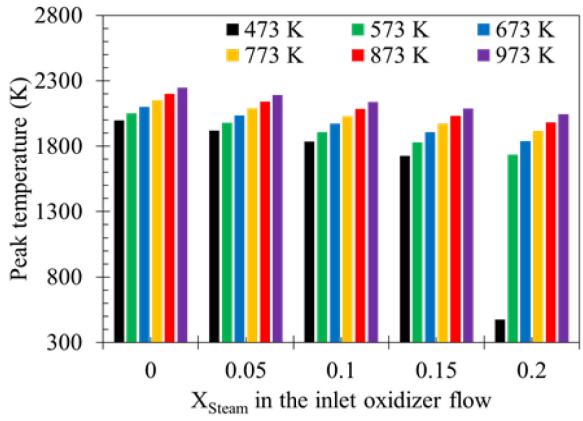

Fig.2a. Variation of peak temperatures of 10%H_2+90%NH_3 and air flames as a function of X_{Steam} at oxidizer temperatures of 473K, 573K, 673K, 773K, 873K, and 973K.

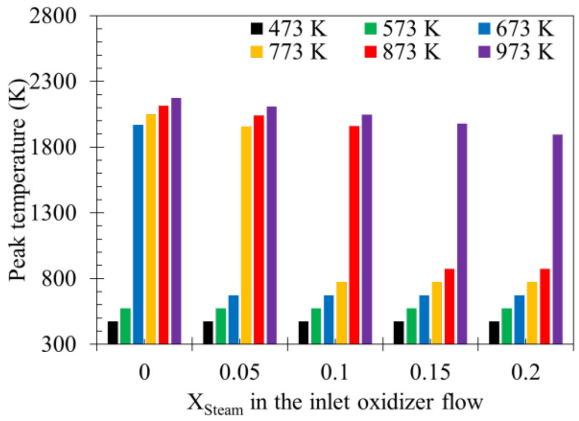

Fig.2b. Variation of peak temperatures for the NH_3-Air+Steam flames as a function of X_{Steam} at oxidizer temperatures of 473K, 573K, 673K, 773K, 873K, and 973K.

Figure 2(b) illustrates the peak temperature for the 100% NH_3 flame with increasing steam to the oxidizer flow. The flames with steam additions of 15% and 20% extinguish for all oxidizer temperatures. The flames with 10% steam addition extinguishes for all temperatures at or below 773K. The flames with 10% steam addition extinguishes for all temperatures at or below 773K and the flames with 5% steam addition extinguish at all temperatures at or below 673 K. of 473 K and 573 K extinguish with and without steam addition. The peak temperatures decrease with increasing addition of steam to the oxidizer flow while oxidizer temperature remains constant. Conversely, the peak temperature increases with increasing oxidizer temperature.

Variation of axial velocities:

Figures 3(a and b) illustrate the variations of axial velocities at different oxidizer temperatures when the mole fraction of ammonia is 0.9 and 1.0, respectively. Lighter shades of different colors representing different temperatures show the variation of mole fractions of steam added. The lightest shades of each color represent a 20% mole fraction of steam added in the oxidizer flow, the darkest one represents the situation with no added steam.

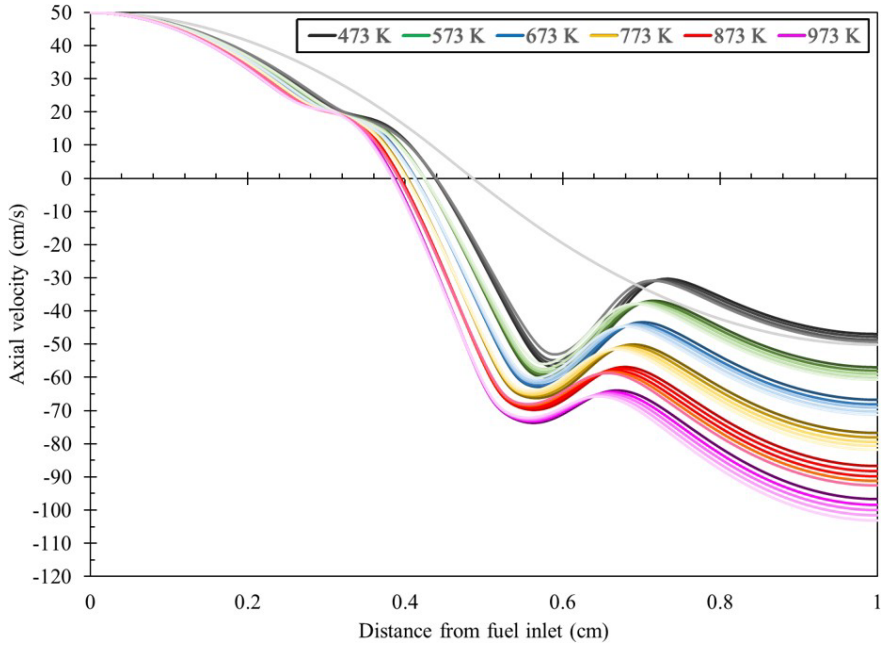

Fig.3a. Variation of axial velocities for the 10% H_2+90% NH_3-Air flames as a function of distance from the fuel inlet at oxidizer temperatures of 473K, 573K, 673K, 773K, 873K, and 973K for increasing X_{H2O} indicated by lighter shade at each oxidizer temperature.

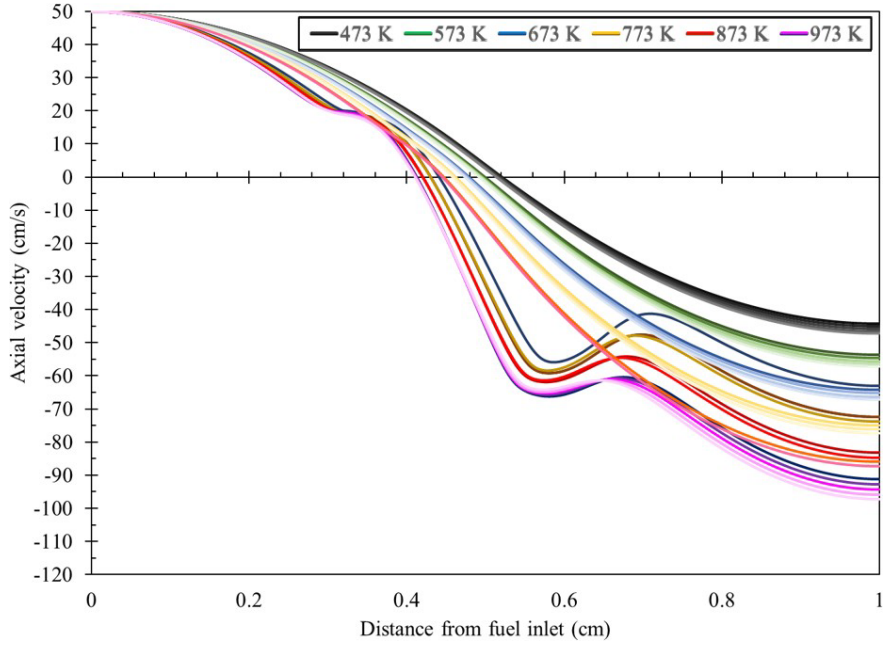

Fig.3b. Variation of axial velocities for the XH_3-Air flames as a function of distance from the fuel inlet at oxidizer temperatures of 473K, 573K, 673K, 773K, 873K, and 973K for increasing X_{H2O} indicated by lighter shade at each oxidizer temperature.

The Left and right sides of both the plots represent the oxidizer inlet side and fuel inlet side, respectively. In the counterflow flame burner, the flame lies at the location where the local minima exist for the variation of the axial velocity curve along the axis of the burner [16]. represents the situation with no added steam. Analyzing both figures, it can be found that with increasing oxidizer temperature, the location of flame shifts towards the fuel side.

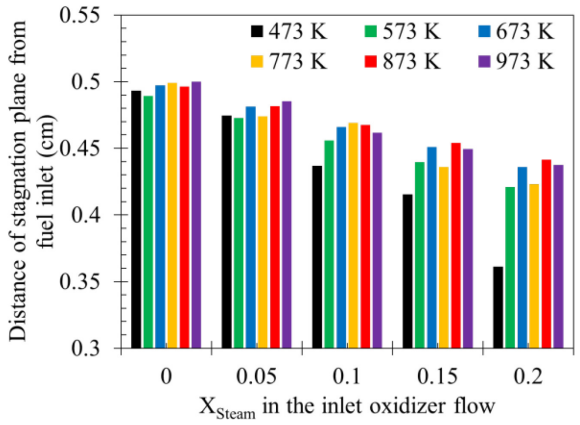

Fig.4a. Location of the stagnation plane from the fuel exit for oxidizer temperatures of 473K, 573K, 673K, 773K, 873K, and 973K as a function of X_{H2O} for the fuel flow X_{NH3} = 0.9. The location of the stagnation plane changes because of the changes in the velocity profiles resulting from the changes in density resulting from combustion.

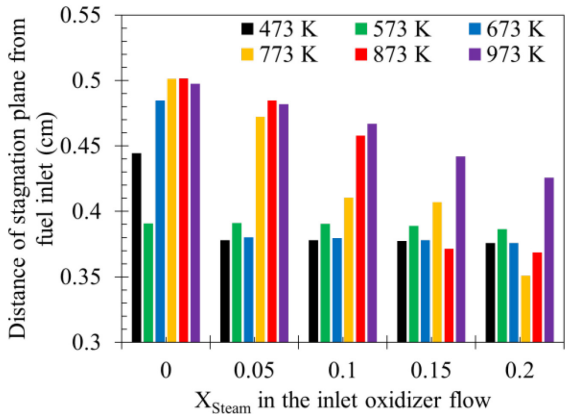

Fig.4b. Location of the stagnation plane from the fuel exit for oxidizer temperatures of 473K, 573K, 673K, 773K, 873K, and 973K as a function of X_{H2O} for the fuel flow X_{NH3} =1 flame. The location of the stagnation plane changes because of the changes in the velocity profiles resulting from the changes in density resulting from combustion.

The distance of the stagnation planes for the NH_3 flames with air containing increasing amounts of steam are illustrated for five values of X_{H2O}. The stagnation planes of the 17 flames that undergo extinction are located relatively close to the fuel exit and approximately at 0.37 cm. The higher temperature flames lead to the stagnation planes moving away from the fuel exit. For all of the cases involving combustion, the stagnation planes are located between 0.45 and 0.5 cm from the fuel exit.

The location of the stagnation plane for the lowest oxidizer temperature remains close to 0.5 cm from the fuel exit for all air temperatures. As the air temperature increases the velocity of air increases and the flames move away from the air inlet and towards the fuel inlet for all steam mole fractions. The flames with higher oxidizer temperatures stabilize closer to the oxidizer inlet. The stagnation plane following extinction is located at 0.355 cm from the fuel exit.

Variation of NO emissions:

NO formation is strongly dependent on the peak temperature, shown in Fig.2 [16]. Figures 5(a) and 5 (b) illustrate the peak mass fraction of NO for the X_{NH3}=0.9 and fuel flow X_{H2}=0.1 flame and the X_{NH3}=1.0 flames. Comparing Fig.5(a) and Fig.5(b), it's noteworthy that introducing steam with a same oxidizer temperature decreases the mass fraction of NO emissions with pure

ammonia-air combustion than 90% ammonia and 10% hydrogen mixture and air combustion. However, the increase in NO formation suggests that air preheat temperatures above 773K should be avoided.

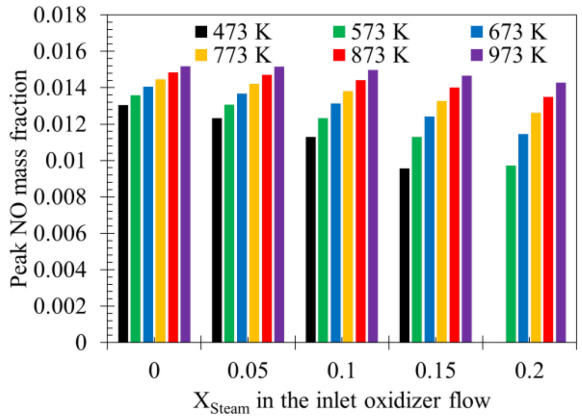

Fig.5a. Peak mass fraction of NO as a function of mole fraction of steam for oxidizer temperatures of 473K, 573K, 673K, 773K, 873K, and 973K for the fuel flow X_{NH3}=0.9 and fuel flow X_{H2}=0.1 flames.

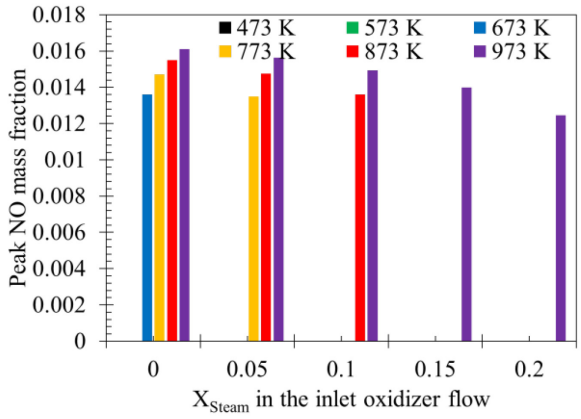

Fig.5b. Peak mass fraction of NO as a function of mole fraction of steam for oxidizer temperatures of 473K, 573K, 673K, 773K, 873K, and 973K for the fuel flow X_{NH3}=1.0.

CONCLUSIONS: A study of opposed flow flames burning NH_3 with small amounts of H_2 with preheated air with different levels of steam addition has shown the possibility of stable combustion for a range of conditions of interest to designers of gas turbine combustors with zero carbon dioxide emissions. Future work will involve comparisons with experiments conducted with temperature and species concentration measurements with coherent anti-Stokes Raman scattering (CARS).

AUTHORS' DETAILS:

Sreetam Bhaduri
Doctoral Candidate
School of Mechanical Engineering
Purdue University, West Lafayette, Indiana – 47907, USA
Email: bhaduri@purdue.edu

Prof. Jay P. Gore
Reilly University Chair Professor
School of Mechanical Engineering
Purdue University, West Lafayette, Indiana – 47907, USA
Email: gore@purdue.edu

REFERENCES:

1. Paraschiv, S., & Paraschiv, L. S. (2020). Trends of carbon dioxide (CO2) emissions from fossil fuels combustion (coal, gas and oil) in the EU member states from 1960 to 2018. Energy Reports, 6, 237-242.
2. Erdemir, D., & Dincer, I. (2021). A perspective on the use of ammonia as a clean fuel: challenges and solutions. International Journal of Energy Research, 45(4), 4827-4834.
3. Yang, W., Dinesh, K. R., Luo, K. H., & Thevenin, D. (2022). Direct numerical simulation of turbulent premixed ammonia and ammonia-hydrogen combustion under engine-relevant conditions. International Journal of Hydrogen Energy, 47(20), 11083-11100.
4. Goldmann, A., & Dinkelacker, F. (2022). Investigation of boundary layer flashback for non-swirling premixed hydrogen/ammonia/nitrogen/oxygen/air flames. Combustion and Flame, 238, 111927.
5. Cellek, M. S. (2022). The decreasing effect of ammonia enrichment on the combustion emission of hydrogen, methane, and propane fuels. International Journal of Hydrogen Energy.
6. Yu, Z., & Zhang, H. (2022). End-gas autoignition and knocking combustion of ammonia/hydrogen/air mixtures in a confined reactor. International Journal of Hydrogen Energy.
7. Kanoshima, R., Hayakawa, A., Kudo, T., Okafor, E. C., Colson, S., Ichikawa, A., ... & Kobayashi, H. (2022). Effects of initial mixture temperature and pressure on laminar burning velocity and Markstein length of ammonia/air premixed laminar flames. Fuel, 310, 122149.
8. Shen, Y., Zhang, K., & Duwig, C. (2022). Investigation of wet ammonia combustion characteristics using LES with finite-rate chemistry. Fuel, 311, 122422.
9. Mashruk, S., Xiao, H., & Valera-Medina, A. (2021). Rich-Quench-Lean model comparison for the clean use of humidified ammonia/hydrogen combustion systems. International Journal of Hydrogen Energy, 46(5), 4472-4484.
10. He, Y., Zou, C., Song, Y., Chen, W., Jia, H., & Zheng, C. (2016). Experimental and numerical study of the effect of high steam concentration on the oxidation of methane and ammonia during oxy-steam combustion. Energy & Fuels, 30(8), 6799-6807.
11. Konnov, A. A. (2009). Implementation of the NCN pathway of prompt-NO formation in the detailed reaction mechanism. Combustion and Flame, 156(11), 2093-2105.
12. Xiao, H., Howard, M., Valera-Medina, A., Dooley, S., & Bowen, P. J. (2016). Study on reduced chemical mechanisms of ammonia/methane combustion under gas turbine conditions. Energy & Fuels, 30(10), 8701-8710.
13. Kumar, P., & Meyer, T. R. (2013). Experimental and modeling study of chemical-kinetics mechanisms for H2–NH3–air mixtures in laminar premixed jet flames. Fuel, 108, 166-176.
14. Ali, H. M. (Ed.). (2020). Hybrid nanofluids for convection heat transfer. Academic Press.
15. Kobayashi, H., Hayakawa, A., Somarathne, K. K. A., & Okafor, E. C. (2019). Science and technology of ammonia combustion. Proceedings of the Combustion Institute, 37(1), 109-133.
16. Turns, S. R. (1996). Introduction to combustion (Vol. 287, p. 569). New York, NY, USA: McGraw-Hill Companies.